Comb Drive Designs With Minimized Levitation

Pablo G. del Corro, Matthias Imboden, David J. Bishop, *Member, IEEE*, and Hernan Pastoriza

***Abstract*— This paper presents two capacitive comb drive designs for electrostatic actuation of MEMS with the aim to eliminate the levitation effect often observed in such systems. By placing a shield over the comb drive fingers, it is possible to balance the electric field and suppress vertical forces while maintaining the desired lateral motion. By optimizing the comb geometry, we demonstrate that our approach is able to reduce the levitation by an order of magnitude and unwanted coupling of motion from out-of-plane to in-plane by a factor of 7 compared with standard comb architectures fabricated using PolyMUMPs technology, without the need of alternating comb finger polarities or additional control electrodes. Levitation was reduced to 160 nm, for 3.6-μm lateral displacement at a driving voltage of 80 V. [2016-0156]**

***Index Terms*— MEMS, comb drives, levitation, actuators.**

I. Introduction

COMB drives [1] are widely used in MEMS devices for linear actuation due to their relative high stroke and force that can be achieved. As the capacitance changes linearly with the displacement along the actuation direction, the force generated in comb drives is proportional to the actuation voltage squared and can hence be easily controlled by a standard voltage source.

In comb drives built using surface micromachining techniques it has been shown [2] that the force exerted to the mobile structure includes not only the desired lateral component, but also a component in the vertical direction, causing the comb to levitate and rise out of the plane. The electric field asymmetry [3] generated by the presence of a ground plane underneath the structure is responsible for this out-of-plane force. Generally speaking, the relative amplitude of the vertical force increases with increasing asymmetry of the electric field above and below the combs.

The levitation effect has been utilized as a mechanism for generating out-of-plane actuation control [6]. However, in general it is an undesirable effect. For one, the out-of-plane motion modifies the simple, linear mechanical response with respect to the voltage squared applied. This is the result of a non-monotonic relationship between the applied voltage squared and the capacitance [7], [8]. Furthermore, the accuracy of MEMS based positioners, that often use comb drives [9], [10], can be compromised.

For high aspect ratio MEMS devices made out of thick SOI wafers the levitation effect can be negligible. SOI processes enables one to remove the substrate and the ground plane beneath the electrically active structure, symmetrizing the electric field and therefore eliminating any levitation effect. This allows for the use of comb drives devices in applications like micro-STMs and mico-AFMs [11]. However, removing the substrate and ground plane is not always an option and will often considerably increases the fabrication complexity.

Thinner devices fabricated from deposition/etch processes such as used in PolyMUMPS [4] or SUMMiT V [5] are strongly affected by levitation. A number of strategies have been developed to reduce this effect. Tang *et al.* [2], [12] proposed the use of alternating the comb finger voltages applied to the fixed electrodes. With this configuration the fringe field in the vertical direction is reduced and as consequence so is the vertical force. However, this approach increases the complexity of the design, requires bi-polar drive electronics and furthermore does not fully eliminate the out-of-plane motion. Imboden *et al.* [13] analyzed the levitation effect in a moving comb and propose replacing the underlying ground plane with an active electrode whose voltage can be tuned to compensate the out-of-plane force. While effective, this approach also includes more complex drive electronics and increases the risk of electrostatic pull in as now the moving combs are attracted to the substrate. Furthermore, when using the combs for sensing purposes the underlying electrode increases the parasitic capacitance and reduces sensing accuracy.

We present two novel design alternatives (and variations thereof) for surface machined comb drives, which by design, reduce the levitation effect by symmetrizing the electric fields above and below the combs. This is accomplished by mirroring the bottom ground plane with a second plane placed above the comb fingers.

In this study we show how to minimize the levitation passively within the design and fabrication constraints of the multi-user PolyMUMPs process provided by MEMSCAP.

II. Displacement Analysis

A comb drive is made up of two parts, an array of fixed fingers anchored to the substrate and another array of

Manuscript received July 5, 2016; revised August 22, 2016; accepted September 29, 2016. This work was supported by the ANPCyT under Grant PICT 0770. The work of D. J. Bishop was supported by the DARPA A2P Program through AFRL under Contract FA8650-15-C-7545. Subject Editor R. T. Howe.

P. G. del Corro and H. Pastoriza are with the Laboratorio de Bajas Temperaturas, Centro Atomico Bariloche, Comision Nacional de Energia Atomica, Instituto Balseiro, Bariloche R8402AGP, Argentina, and also with the Consejo Nacional de Investigaciones Cientificas y Tecnicas, Buenos Aires C1033AAJ, Argentina.

M. Imboden is with the Microsystems for Space Technologies Laboratory, École Polytechnique Fédérale de Lausanne (EPFL), 2002 Neuchâtel, Switzerland.

D. J. Bishop is with the Department of Electrical and Computer Engineering, Boston University, Boston, MA 02215 USA, and also with the Department of Physics, Boston University, Boston, MA 02215 USA.

Color versions of one or more of the figures in this paper are available online at http://ieeexplore.ieee.org.

Digital Object Identifier 10.1109/JMEMS.2016.2614965

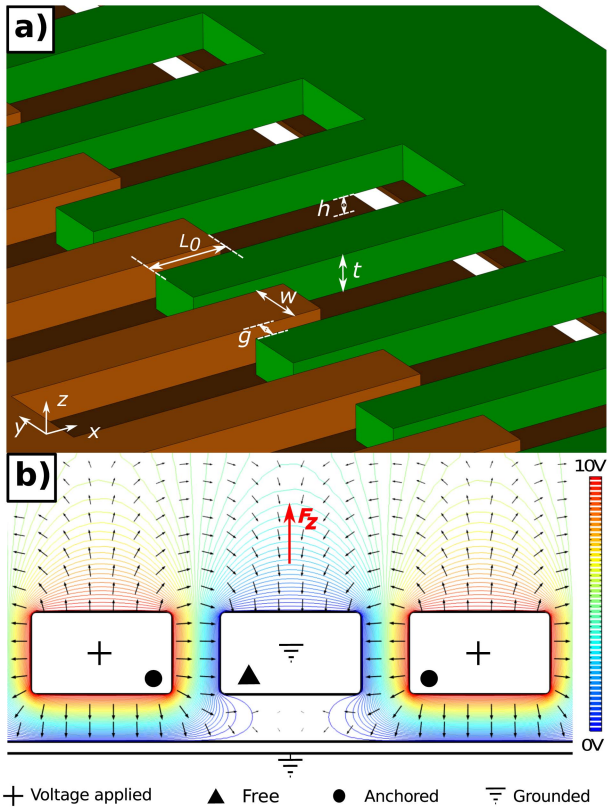

Fig. 1. a) 3D view of a generic interdigitated comb drive structure. b) Slice through the combs in the overlapped area L_0 illustrating the asymmetric electric field (arrows) and electric potential distribution (colored lines), resulting in a levitating force F_z.

interdigitated fingers suspended by springs. The fingers of width w and thickness t are separated by a gap g and overlap by an initial length L_0 as is shown in figure 1 a). Typically, a grounding plane shorted electrically to the moving structure is placed underneath all the fingers at a height h. This avoids unwanted charge accumulation in the substrate [12] or a floating potential which could adversely affect the stability of the electromechanical response.

By applying a voltage V to the fixed combs array, an electrostatic force acts on the mobile structure given by:

$$\vec{F_E} = \frac{1}{2}\vec{\nabla} C V^2 \tag{1}$$

where C is the total capacitance of the comb drive. This force is balanced by springs suspending the mobile structure as described by Hooke's law.:

$$\vec{F_M} = -\mathbf{k}\vec{d} \tag{2}$$

with $\mathbf{k}$ the spring constant tensor and $\vec{d}$ the spatial displacement.

In an ideal system the resulting force acts only parallel to the fingers, resulting in a displacement linear to the square of the applied voltage ($\frac{dC}{dx} = $ constant and $\frac{dC}{dy} = \frac{dC}{dz} = 0$). In typical systems however, there is an asymmetry in the electrostatic boundary conditions produced by the ground plane beneath the fingers. This results in an asymmetry of the electric field that induces a force normal to the plane of the substrate F_{Ez} (see figure 1 b)). Consequently, the mobile structure levitates, maximizing the electrical potential energy between fingers (increasing its capacitance) [7] and consequently the capacitance becomes a function of z in addition to x.

In the case of a minimal vertical mechanical restoring force, the maximal levitation displacement would be given when the electric force $F_{Ez} = \frac{1}{2}\frac{\partial C}{\partial z}V^2$ is equal to zero.

Using the coordinate system of figure 1 a), the electric force components for the lateral (x) and vertical (z) displacements can be expressed as [2]:

$$F_x = \frac{1}{2}\frac{dC}{dx}V^2 \qquad F_z = \frac{dc}{dz}\frac{L_0}{2}\frac{(z_m - z)}{z_m}V^2. \tag{3}$$

Here, c is the capacitance per unit of length, $\frac{dc}{dz}$ the gradient of the capacitance along the z-axis per unit length, z_m is the asymptotic value that fingers will reach for the given geometry, and z the vertical displacement.

From these equations the expressions for lateral and vertical displacements of a comb drive can be approximated as:

$$x = \frac{1}{2k_x}\frac{dC}{dx}V^2 \simeq \frac{\eta}{2k_x}\frac{N\epsilon_0 t}{g}V^2 \tag{4}$$

and

$$z = \frac{\frac{z_m}{2}\frac{dc}{dz}L_0 V^2}{k_z z_m + \frac{1}{2}\frac{dc}{dz}L_0 V^2}. \tag{5}$$

k_x is the spring constant in x direction, η describes the electromechanical coupling factor for the given geometry, N is the number of fingers, ϵ_0 is the permittivity of vacuum and k_z is the spring constant in z direction.

As described in full by Imboden *et al.* [13] x and z are interdependent. The levitation will be affected by the lateral displacement as the overlap between fingers changes from L_0 to $L_0(1 + x/L_0)$, thus by combining equations 4 and 5 one obtains [13]:

$$z = \frac{\frac{z_m}{2}\frac{dc}{dz}L_0(1 + \frac{dC}{dx}\frac{V^2}{2k_x L_0})V^2}{k_z z_m + \frac{1}{2}\frac{dc}{dz}L_0(1 + \frac{dC}{dx}\frac{V^2}{2k_x L_0})V^2} \tag{6}$$

or in terms of displacement x:

$$z = \frac{\frac{z_m}{2}\frac{dc}{dz}L_0(1 + \frac{x}{L_0})V^2}{k_z z_m + \frac{1}{2}\frac{dc}{dz}L_0(1 + \frac{x}{L_0})V^2} \tag{7}$$

The lateral displacement will also be affected by levitation due the change of $\frac{dC}{dx}$ with levitation [7], increasing the effective finger thickness.

III. Designs

The PolyMUMPs process used for the fabrication of our structures offers the possibility to design MEMS devices using three layers of highly doped poly-silicon and a single metal layer [4]. The conductive substrate is isolated from the three layers by a 0.6 μm thick silicon nitride layer. The first poly silicon layer, Poly0, is 0.5 μm thick and must be anchored to the nitride. The next poly silicon layer, Poly1 (2 μm thick), is separated from Poly0 by a 2 μm thick silicon oxide sacrificial layer. A second oxide layer 0.75 μm thick spaces the Poly1 layer from the top 1.5 μm thick Poly2 layer. Poly1 and Poly2

can be anchored to the substrate (and/or to each other). A final gold layer is placed on the Poly2 layer and is used to form a high quality electrical connection to the MEMS.

Considering that the levitation of the comb drives is a consequence of the electric fringe field asymmetry, two design approaches can be used to reduce the vertical actuation. The first one is to physically remove the underline ground plane which is difficult to do using standard surface micro fabrication methods. An alternative approach to symmeterize the electric field is to mirror the bottom ground plane with a second ground plane placed above the comb fingers. This is the approach discussed in this work.

Two different options have been evaluated. One, referred to as the *fully-shielded design*, a continuous grounded plane is placed on top of the mobile fingers of the comb drive. Due to the fixed number of poly-silicon layers available, this guard line is fabricated adjacent to the drive and then flipped over the top of the comb drive after the release. To ensure symmetric fringe fields the height above the fingers must match the spacing below the fingers.

A second approach, termed *partially-shielded design*, is based on grounded fingers placed above the static, charged actuation fingers of the comb acting as a screen of the electric field. In this approach the last poly-silicon layer is used to build the shield. Two strategies to achieve this partial-shield are presented.

The task presented here is to maximize the symmetry of the fringe field while working within the process constraints and fabrication tolerances: This includes a minimum feature size of two microns and alignment tolerances of order one micron. A robust design would enable an efficient, easily implementable solution to suppress the levitation effect. The next sections describe the proposed designs and is followed by their implementation and evaluation.

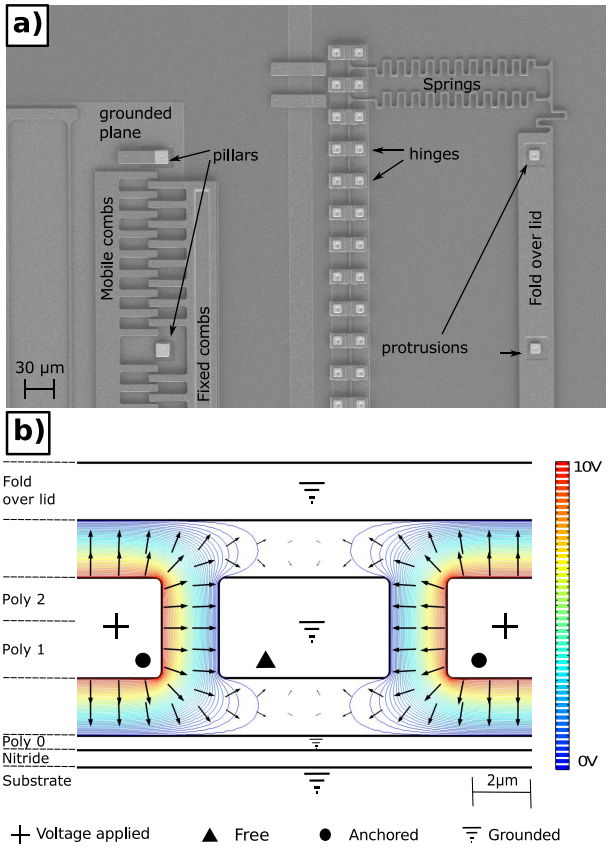

Fig. 2. a) SEM image of fully-shielded design after released, the shield has not been flipped. b) Finite element simulation of the electrical potential distribution (colored scale) and field lines (black arrows) of the fully-shielded design. A PolyMUMPs process layers reference is included on the left side of the simulation (dashed lines).

A. Fully-Shielded Design

This design is a standard comb drive with the addition of four pillars placed between fingers of the comb array. For this design the anchored and mobile fingers are built using the Poly1 and Poly2 layer together. A rectangular shield with protrusions is fabricated adjacently and tethered by a spring and hinge system (see figure 2 a)). Using the PolyMUMs layers, the pillars made of Poly1, Poly2 and gold are level with the top of the static combs. The protrusions on the shield are constructed to be of the same height as the gap between the grounded plane and the comb fingers. After the release the shield can be flipped over the combs, symmetrically encapsulating the mobile fingers. Pillars and protrusions are aligned, so when the shield is flipped over the combs the protrusions sit on the pillars. In this way the same 2 μm gap can be ensured above and below the comb fingers.

To symmeterize the fringe fields and eliminate the vertical force, the shield must be at the same potential as the mobile fingers and ground plane. By anchoring the pillars to the grounded plane, the mechanical contact between pillars and protrusions will ensure an electrical short between the shield and ground plane as well. As the applied voltage increases, the shield is attracted to the top surface of the comb fingers improving both the mechanical and electrical contact. Adjacent pillars must be sufficiently close to ensure minimal mechanical deformation of the shield. Too many pillars reduce the lateral force of the drive and increases edge effects. In this case sets of 8 combs per pillar were fabricated.

Figure 2 b) is a simplified cross section 2D simulation of this design showing how the electric potential is symmetric above and below the combs (colored contour lines). Electric field lines are represented by the arrows. Ideally, this design would fully eliminate the levitation effect, since the net force in the vertical direction acting on the mobile fingers vanishes.

B. Partially-Shielded Design

With the three level process provided by PolyMUMPs the only way to create a continuous symmetric top is by placing (or flipping) the shield after the release. This requires manual post processing steps which are not scalable, and hence ill-suited for mass production. A partially-shielded comb drive was designed as a way to avoid this extra step. A Poly2 grounded structure is suspended over the charged static combs and is used as a screen of the electric fringe field. The electric field lines above the fingers are attracted to the top shield and behave similarly to the bottom ground plane. The fringe fields

above the mobile fingers are diminished and the vertical forces are suppressed.

For this design the anchored and mobile fingers are built using the Poly1 layer. As the Poly2 layer is now used for shielding, the fingers are thinner than in the Fully-Shielded design. The gap between the fingers and the partial shield is defined by the 0.75 μm second sacrificial silicon oxide layer (Oxide2). The width of the top screen must be significantly narrower than the finger width to allow for fabrication tolerances. In this case the screen is designed two microns narrower than the fingers. As the top gap is smaller than the lower gap a narrower finger can still effectively suppress the fringe fields. The distance between the bottom surface of fingers and the grounded plane h is the thickness of the first silicon oxide sacrificial layer (Oxide1 $= 2\ \mu m$). This height can be reduced by using the dimple mask, reducing h by 0.75 μm to 1.25 μm. For the data presented here, the use of a dimple mask will be indicated with the label "(dimple)", otherwise no dimple mask is used.

Two slightly different partially shielded designs are presented next:

1) Continuous Bottom Ground Plane: For this design, referred to as *Partially-Shielded A*, the Poly0 layer is a continuous ground plane beneath all comb fingers.

A SEM image of Partially-Shielded A (dimple) structure is shown in figure 3 a). The alignment mismatch of the PolyMUMPs process can be observed in the offset of the fixed fingers and the partial shield ($\sim$1 μm). The electric field, simulated for a perfectly aligned cross section, can be seen in figure 3 b).

2) Segmented Bottom Ground Plane: As described by Tang *et al*. [2], levitation effects can be reduced by modifying the plane underneath the fingers.

In this design, referred to as Partially-Shielded B, the ground plane below the fingers is segmented. Each segment is centered to and held at the same potential as the finger above it. Maximal electric field symmetry is predicted for fully enclosed segments. Hence, allowing for fabrication tolerances, the poly0 elements are narrower than the fingers. A 2D finite element simulation of the electric potential and field lines is depicted in figure 4. The fingers are now deformed due to the print through effect of the fabrication process. Some fabrication processes include planarization between depositions but this significantly increases the fabrication complexity.

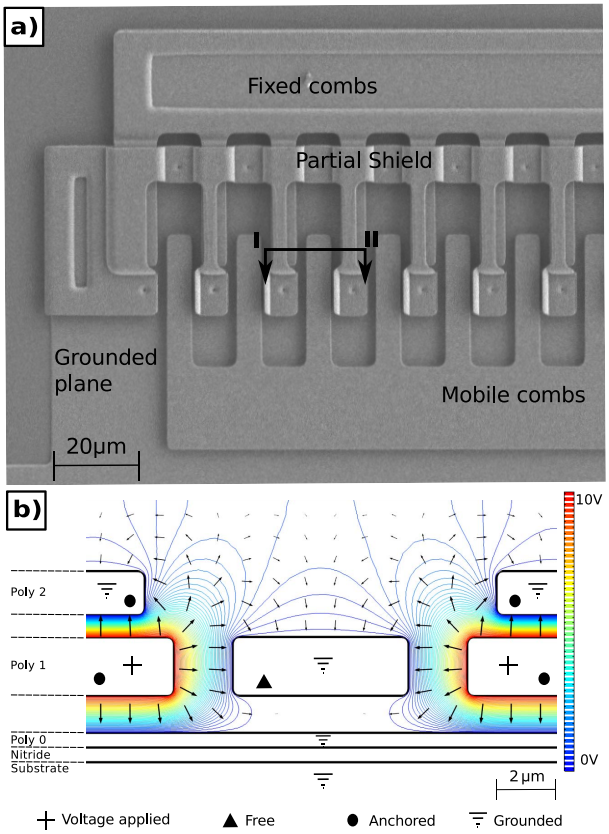

Fig. 3. a) SEM image of the partially-shielded device with a continuous bottom ground plane(dimple). b) Finite element simulation of the electrical potential (colored scale) of an ideal cross section (defined by I and II) of the actuator in the overlapping region. Electric field distribution in z is represented by black arrows. A PolyMUMPs process layers reference is included on the left side of the simulation (dashed lines).

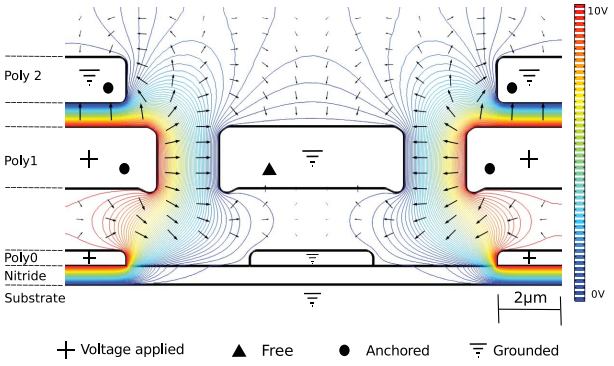

Fig. 4. Finite element simulation of the electric potential lines of a cross section for the partially-shielded B design (colored scale). Electric field lines are illustrated by black arrows. A PolyMUMPs process layers reference is included on the left side of the simulation (dashed lines).

IV. Experiments and Results

Three devices were fabricated and tested: a standard comb drive for comparative purposes, the fully-shielded design expected to have the best performance but requires post release assembly and the partially-shielded design A (dimple). The Partially-Shielded A design (without dimple mask) as well as the Partially-Shielded B have not been fabricated but are straight forward to implement and have hence been included in the analysis and evaluation below using finite element simulations.

For all cases the combs are suspended by the same folded flexure spring design. This way k_x and k_z are held constant for all devices. Furthermore, the number of fingers N (63), their width w (6 μm), length L (32 μm) and initial overlap L_0 (8 μm) are the same for each design.

Figure 5 shows an optical micrograph of the fully-shielded comb drive with the shield flipped over the comb fingers using a micro-manipulator.

All measurements of the levitation and lateral displacement were made using a Wyko NT1100 optical profiler. The origin is taken to be the zero voltage position for both vertical (z)

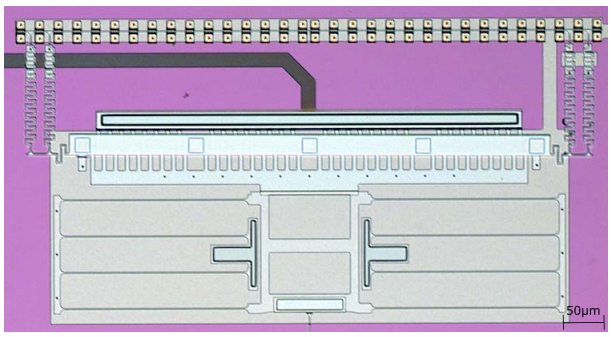

Fig. 5. Optical micrograph of the fully-shielded comb drive with the shield flipped into place.

and horizontal (x) displacement. All motion occurs in the $x-z$ plane. Plots of the levitation displacement as a function of the voltage squared and as a function of the lateral displacement for all devices are depicted in figure 6 a) and c) respectively. Figure 6 b) and d) represent the lateral displacement and the levitation to lateral displacement ratio as a function of the voltage squared respectively. The applied voltage ranges from 0 to 80 V in 10 V increments.

The experimental data is fitted to equations 6 and 7 to obtain the electromechanical coupling strength in x and z as well as the maximum levitation reached (z_m). The results are summarized in table I, where the simulated maximum levitation is also included for comparison.

It can be seen in figure 6 that the levitation is reduced considerably for both devices proposed by this work. As expected the fully-shielded device before the flip-over of the shield behaves essentially identically to the standard comb. After the assembly the device becomes fully shielded and the levitation is limited to 160 nm, a factor of 9.72 lower than the standard comb. The fact that levitation it is not canceled completely can be attributed to imperfections in the fabrication such as the tolerance of the polysilicon and the sacrificial layers, edge effects as well as a slight deformation of the top shield at higher drive voltages.

As predicted, the lateral displacement is affected as well. In order to symmetrize the electric field given the fabrication constraint, a reduction in the total capacitance C and $\frac{dC}{dx}$ could not be avoided. In addition to lowering the vertical equilibrium position, the new designs presented also significantly reduce the vertical electromechanical coupling (see Table I). The lateral electromechanical coupling is also reduced and consequently the lateral displacement as well, as illustrated in figures 6 b) and c). Figure 6 b) also shows that the lateral displacement in a standard comb drive is strongly affected by levitation at low voltages. This $x-z$ coupling is almost eliminated by the proposed design as is illustrated by the reduction in the electromechanical coupling ratio (see Table I).

It is important to note that the reduction in z_m is independent of the maximum applied voltage. Hence as the drive voltage increases the z/x displacement ratio falls off dramatically, this is clearly illustrated in figure 6 d).

The partially shielded design suffers the greatest loss on lateral electromechanical coupling as the comb finger thickness has been reduced from 3.5 μm to 2 μm. Even the fully-shielded design results in a 50% reduction of the lateral electromechanical coupling strength, an illustration of the contribution of fringe fields to the capacitance of comb structures with high gap/thickness ratios. The loss in lateral motion can be compensated by increasing the drive voltage by a factor of approximately $\sqrt{2}$, softening the spring constants, and/or by increasing the number of comb fingers.

The partially-shielded A (dimple) device reduces the levitation to within similar values as reported in [13]. Regarding the lateral displacement, [13] improves the performance by approximately 30% with respect to a standard comb drive, while our design reduces lateral displacement by 65%. Nevertheless, as is explained above, there are several ways to compensate for this loss of lateral displacement. On the other hand, the fully shielded device can be compared to data of [12]. In both cases levitation has been reduced by an order of magnitude and the lateral displacement is approximately halved. It should also be noted that the levitation control schemes discussed in [12] and [13] both require additional voltage electrodes and corresponding driving circuit, where the solution presented here requires no such increase in complexity.

To validate the experimental data obtained, the force density along the vertical axis with respect to the vertical position of the mobile fingers was simulated. The results are depicted in figure 7. In addition to the fabricated devices, the simulations include the dimple free partially-shielded A designs and the partially-shielded B designs (segmented ground plane). The zero crossing of the simulation corresponds to the height of the combs if no restoring force is present. As the levitation saturates for high drive voltages this position corresponds to the maximum levitation observed experimentally. The discrepancies between simulation and experimental data can be explained by imperfect fabrication and edge effects of the finite comb. The partially-shielded B design predicts a levitation of only 70 nm without the need for post fabrication assembly, rivaling the ideal situation (zero levitation) shown in 7 by the fully-shielded design. Figure 7 also shows that the dimple free design predicts less levitation than the dimpled design.

The simulations also allows for efficient modeling of the robustness of the predicted levitation. In particular one may want to know, given the processing tolerances, what resulting levitation range should be expected. For this analysis the tolerances of the PolyMUMPs are taken into account. This includes variations of the layer thicknesses [4] as well as alignment accuracies.

Table II shows the simulations performed to evaluate the robustness (or sensitivity to fabrication tolerances) for the fully shielded, the partially shielded A and the partially shielded B designs. No dimpled devices were included for this simulation since dimple free design predicts less levitation. For all cases the strongest dependency is observed with regards to changes in the thickness of the oxide 1 layer, which determines the height (h) of the combs above the bottom plane. Specifically, decreasing the thickness of oxide 1 will increase the levitation by 125 nm, 60 nm and 50 nm for the fully shielded design, the partially shielded A design and partially shielded B design respectively.

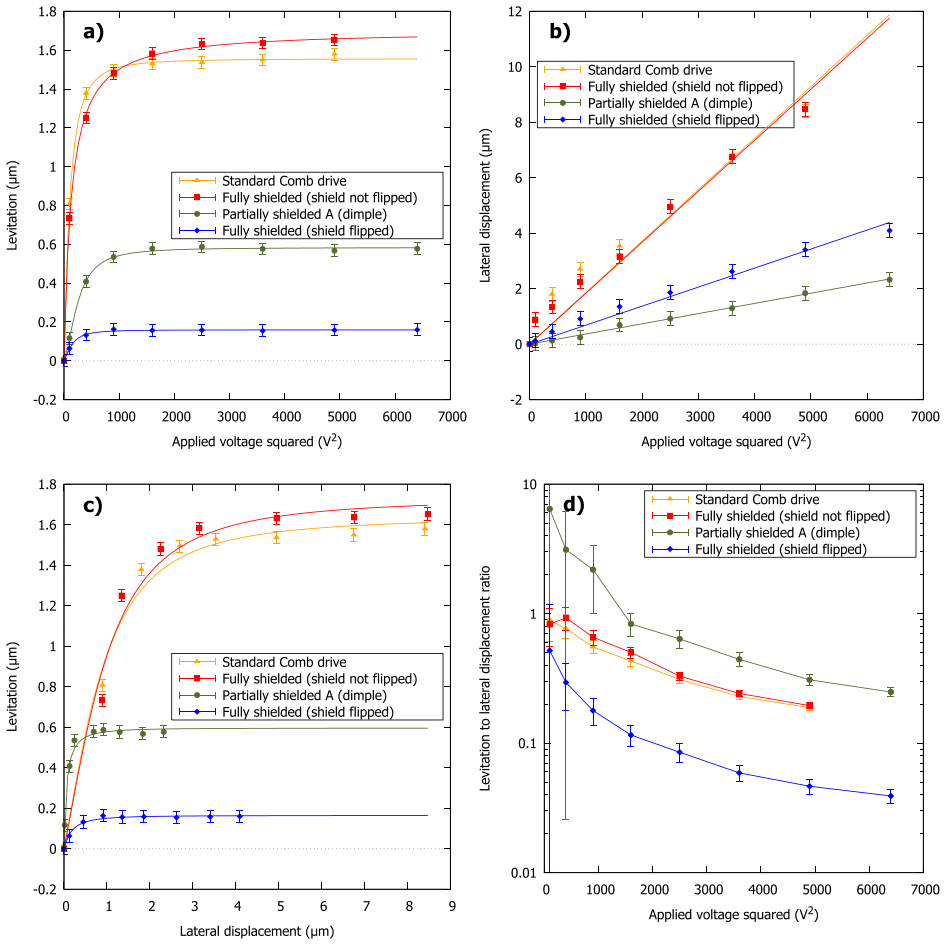

Fig. 6. a) Levitation vs. drive voltage squared for designs with his respective fits (lines). b) Lateral displacement vs. drive voltage squared for all designs. The liner fit appropriates the idealized response, most valid as the levitation vanishes. After the levitation saturates the lateral displacement becomes more precisely proportional to V^2. c) Comparison of vertical and lateral displacement for all the devices fabricated. d) Levitation to lateral displacement ratio vs. drive voltage squared.

TABLE I

EXPERIMENTAL AND SIMULATION FITTING PARAMETERS

Parameters	Standard / Fully Shielded (shield not flipped)	Partially Shielded A (dimple)	Fully Shielded
z_m [μm]	1.555 1.288*	0.583 0.45*	0.160 0*
x coupling** [nm/V^2]	1.9	0.368	0.68
z coupling** [nm/V^2]	12.75	0.758	0.64
z/x coupling ratio**	6.71	2.06	0.94

(*) simulation result.
(**) The coupling and coupling ratio is quoted for V = 0.

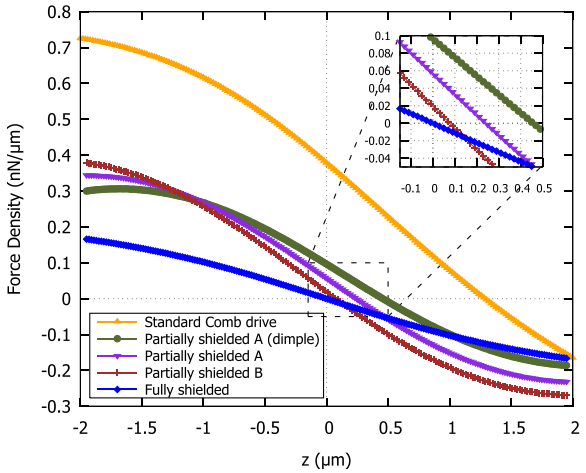

Fig. 7. Simulation of lateral force density at a given drive voltage (10 V) in the overlapped region L_0 as a function of comb finger offset. Inset: Close-up view of the zero crossing, corresponding to the expected levitation amplitude.

Partially shielded A and partially shielded B designs are more robust to layer tolerances than the fully shielded design. As the fully shielded design relies on exact symmetry to maintain zero vertical displacement, it is not surprising that deviations from the ideal can lead to significant shifts of the equilibrium position. Consequently, it can be shown that thickness variations of 100 nm in Poly2 and 60 nm in the Metal layers can together lead to levitation changes of 80 nm for the fully shielded device, while the same fabrication variations predict levitation shifts of less than 10 nm for the other designs. Given the known tolerance of the Poly-MUMPs fabrication process the 160 nm of levitation observed

TABLE II

SIMULATED CONTRIBUTION TO THE LEVITATION REACHED FOR THE MOST SIGNIFICANT TOLERANCES AND ALIGNMENT MISMATCHES

Parameters	Fully Shielded (0 nm)*	Partially Shielded A (230 nm)*	Partially Shielded B (70 nm)*
± 250 nm Oxide1 ± 100 nm Poly2 ± 80 nm Oxide2 ± 60 nm Metal	± 125 nm ± 50 nm not used ± 30 nm	± 60 nm ± 5 nm ± 3 nm not used	± 50 nm ± 6 nm ± 10 nm not used
Poly0 shifted by 1 μm Poly2 shifted by 1 μm Poly0 and Poly2 shifted by 1 μm same direction Poly0 and Poly2 shifted by 1 μm opposite direction	no effect no effect no effect no effect	no effect - 15 nm no effect no effect	- 15 nm - 8 nm - 50nm - 6 nm

* expected levitation reached at zero tolerance and alignment errors.

experimentally can be explained by deviations from the ideal geometry.

Table II also shows that for the partially shielded B design misalignment between poly silicon layers can even improve on the perfectly aligned scenario (zero tolerance and alignment errors). One consideration not included in the simulation is the effect of leaving insulating gaps beneath a charged comb finger. This can introduce instabilities as charges get trapped on the surface of the nitride, and lead to mechanical instabilities or fluctuations in the drive performance [12], [14]. The Partially shielded A design is predicted to be the most robust design with regards to layer thickness tolerances and is almost insensitive to errors in alignment, and hence is the most reliable design.

V. CONCLUSION

In this work we have shown that it is possible using design considerations alone to significantly reduce the effect of levitation in surface micro-machined comb drives. This reduction can be accomplished without increasing the complexity of the electrical drive (such as pull in electrodes or alternate polarity comb fingers). These designs are based on multi project wafer fabrication processes of a commercial foundry, and the method can be expanded to other similar planar fabrication processes. Simulations are used to illustrate the effect of fabrication errors and indicate that the approach is robust within manufacturing tolerances. The lower lateral electro-mechanical coupling can be compensated with the use of higher actuation voltages, softening the spring constants or increasing the number of comb fingers. The results prove that levitation can be almost fully eliminated and that the levitation to lateral displacement coupling ratio can be significantly reduced, allowing improved performance of comb drive devices where accurate lateral displacement is required (such as nano-positioners, accelerometers and gyroscopes) and also improved performance and sensitivity for its capacitive position sensing.

ACKNOWLEDGMENT

P. G. del Corro would like to thank the fellowship from CONICET.

REFERENCES

[1] R. Legtenberg, A. W. Groeneveld, and M. Elwenspoek, "Comb-drive actuators for large displacements," *J. Micromech. Microeng.*, vol. 6, no. 3, p. 320, 1996. [Online]. Available: http://stacks.iop.org/0960-1317/6/i=3/a=004

[2] W. C. Tang, M. G. Lim, and R. T. Howe, "Electrostatically balanced comb drive for controlled levitation," in *IEEE 4th Solid-State Sens. Actuator Workshop Tech. Dig.*, Jun. 1990, pp. 23–27.

[3] H. Hammer, "Analytical model for comb-capacitance fringe fields," *J. Microelectromech. Syst.*, vol. 19, no. 1, pp. 175–182, Feb. 2010.

[4] A. Cowen, B. Hardy, R. Mahadevan, and S. Wilcenski. *PolyMUMPs Design Handbook*, accessed on 2011. [Online]. Available: http://www.memscap.com/data/assets/pdf_file/0019/1729/PolyMUMPs-DR-13-0.pdf

[5] Sandia National Laboratories. *SUMMiT V Design Manual*, accessed on 2012. [Online]. Available: http://www.sandia.gov/mstc/assets/documents/design_documents/SUMMiT_V_ Dmanual.pdf

[6] A. P. Lee, C. F. McConaghy, P. A. Krulevitch, E. W. Campbell, G. E. Sommargren, and J. C. Trevino, "Electrostatic comb drive for vertical actuation," in *Proc. SPIE*, Sep. 1997, pp. 109–119.

[7] W. M. van Spengen and E. C. Heeres, "A method to extract the lateral and normal components of motion from the capacitance change of a moving MEMS comb drive," *J. Micromech. Microeng.*, vol. 17, no. 3, p. 447, 2007. [Online]. Available: http://stacks.iop.org/0960-1317/17/i=3/a=005

[8] W. M. van Spengen and T. H. Oosterkamp, "A sensitive electronic capacitance measurement system to measure the comb drive motion of surface micromachined MEMS devices," *J. Micromech. Microeng.*, vol. 17, no. 4, p. 828, 2007. [Online]. Available: http://stacks.iop.org/0960-1317/17/i=4/a=021

[9] M. Imboden *et al.*, "Atomic calligraphy: The direct writing of nanoscale structures using a microelectromechanical system," *Nano Lett.*, vol. 13, no. 7, pp. 3379–3384, 2013, [Online]. Available: http://dx.doi.org/10.1021/nl401699w

[10] M. Imboden *et al.*, "Building a fab on a chip," *Nanoscale*, vol. 6, no. 10, pp. 5049–5062, 2014. [Online]. Available: http://dx.doi.org/10.1039/C3NR06087J

[11] Y. Xu, N. C. MacDonald, and S. A. Miller, "Integrated micro-scanning tunneling microscope," *Appl. Phys. Lett.*, vol. 67, no. 16, p. 2305, 1995.

[12] W. C. Tang, M. G. Lim, and R. T. Howe, "Electrostatic comb drive levitation and control method," *J. Microelectromech. Syst.*, vol. 1, no. 4, pp. 170–178, Dec. 1992.

[13] M. Imboden, J. Morrison, E. Lowell, H. Han, and D. J. Bishop, "Controlling levitation and enhancing displacement in electrostatic comb drives of MEMS actuators," *J. Microelectromech. Syst.*, vol. 23, no. 5, pp. 1063–1072, Oct. 2014.

[14] H. R. Shea *et al.*, "Effects of electrical leakage currents on MEMS reliability and performance," *IEEE Trans. Device Mater. Rel.*, vol. 4, no. 2, pp. 198–207, Jun. 2004.

Pablo G. del Corro is currently pursuing the Ph.D. degree in engineering sciences with the Instituto Balseiro, Argentina. His thesis was on electrical signal detection and control circuits for MEMS sensor and actuators. He is also an electronic engineer with the National University of Santiago del Estero, Argentina.

Matthias Imboden received the Diploma (M.S.) degree in theoretical physics from Bern University in 2004 and the Ph.D. degree from Boston University in 2012 with a focus on diamond nano-electromechanical resonators: dissipation and superconductivity. He is currently with EPFL, Switzerland, as a Marie Skłodowska-Curie Fellow. His research focuses on micro and nanoelectromechanical systems for both research and technology development, nanoscale fabrication, quench condensed superconductivity, tunable plasmonics, smart lighting systems, and mechanobiology. He is a member of the American Physics Society and serves on the EuroEAP Outreach and Dissemination Committee.

David J. Bishop (M'11) received the B.S. degree in physics from Syracuse University in 1973, and the M.S. and Ph.D. degrees in physics from Cornell University in 1977 and 1978, respectively. He joined the AT&T-Bell Laboratories Bell Labs in 1978 as a Post-Doctoral Member of Staff and became a Member of the Technical Staff in 1979. In 1988, he was made a Distinguished Member of the Technical Staff and later he was promoted as the Department Head, Bell Laboratories. He was the President of Government Research and Security Solutions with Bell Labs, Lucent Technologies. He was the Chief Technology Officer and Chief Operating Officer with LGS, the wholly-owned subsidiary of Alcatel-Lucent dedicated to serving the U.S. federal government market with advanced research and development solutions. He is currently the Head of the Division of Materials Science and Engineering, Boston University, a Professor of Physics, and also a Professor of Electrical Engineering. He is a Bell Labs Fellow and in his previous positions with Lucent served as a Nanotechnology Research VP for Bell Labs, Lucent Technologies, and the President of the New Jersey Nanotechnology Consortium and the Physical Sciences Research VP. He is a member and a fellow of the American Physical Society, and a member of the MRS. He was a recipient of the APS Pake Prize.

Hernan Pastoriza received the Ph.D. degree in physics from the Institutbo Balseiro in 1994. He held post-doctoral positions with Leiden Univerisity and Neuchtel University. He is currently a Principal Researcher with CONICET, a Researcher with CNEA, and also a Professor with the Instituto Balseiro. He has over 50 publications in condensed matter physics, applied physics, and microsensors. Since 2002, he has been involved with the development of microelectromechanical systems for superconductivity research, satellite sensors, and biomedical sensors.